National Synchrotron Radiation Research Center

Soft X-ray Absorption and Resonant Scattering

Di-Jing Huang *djhuang@nsrrc.org.tw*

Nat'l Synchrotron Radiation Research Center, Taiwan
Dept. of Physics, Nat'l Tsing Hua University, Taiwan

Chairon 2007, SPring8, Japan
Sept. 16

1

Electromagnetic Spectrum

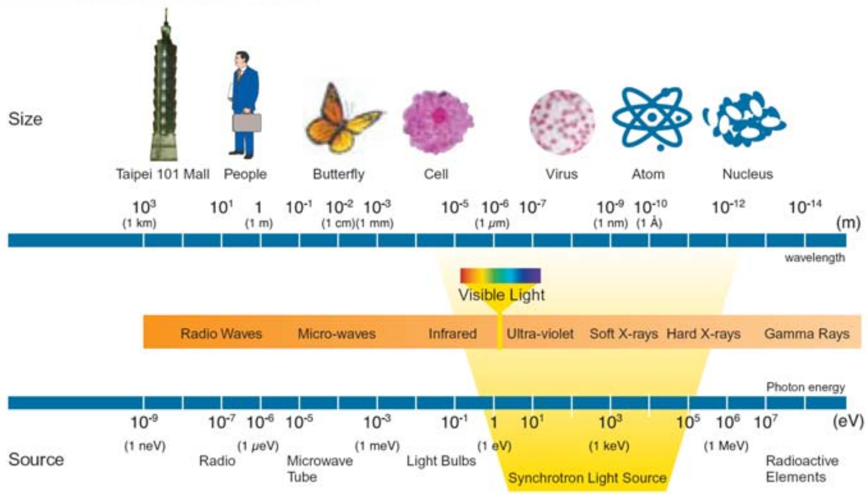

Soft x-ray: 250 eV ~ a few keV

2

Interaction of photons with matter:

Photoelectric effect
Photoabsorption
Scattering / diffraction

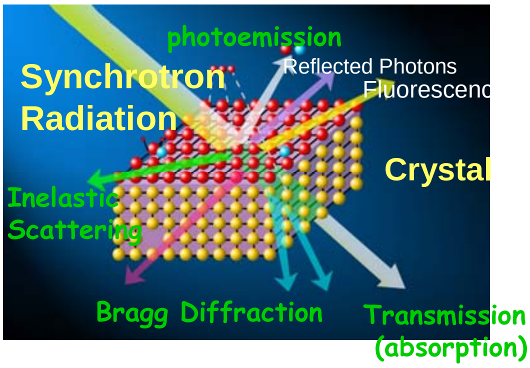

- lattice structure: arrangement of atoms
- electronic states
- magnetic order
- excitations (electronic states or phonons)

3

Soft X-ray Absorption and Resonant Scattering

1. Basics of x-ray scattering and absorption
2. Soft X-ray Absorption
   - Experimental Setup
   - Applications
     - Chemical analysis
     - Orbital polarization
     - Magnetic Circular Dichroisn
3. Resonant Soft X-ray Scattering
   - Basics
   - Examples
     - Verwey transition of Fe_3O_4
     - Charge-Orbital ordering and Quasi-2D magnetic ordering of $La_{0.5}Sr_{1.5}MnO_4$

4

X-ray absorption

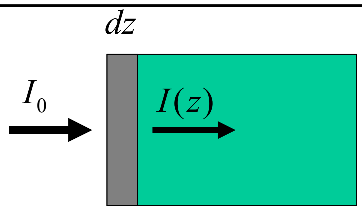

$$\frac{d\sigma}{d\Omega} = \frac{W_{\Delta\Omega}}{\Phi_0 \Delta\Omega}$$

$$\Phi_0 = \frac{I_0}{A}$$

absorption coefficient μ

$$-dI(z) = \mu\, I(z)\ dz$$

$$\frac{\mathbf{d}\boldsymbol{I}(\mathbf{z})}{\mathbf{dz}} = -\mu\, \mathbf{I}(\mathbf{z}) \qquad I(z) = I_0 e^{-\mu z}$$

# of absorption events $W = I(z)\underbrace{\rho dz}_{\text{\# of atoms/area}}\sigma_a = I(z)\mu dz$

$$\mu = \rho\sigma_a$$

absorption cross section

$$n \equiv 1 - \delta + i\beta \qquad (\alpha \text{ and } \beta \text{ are real numbers})$$

The wave propagating in the medium is

$$E_0 e^{i(nkz)} = E_0 e^{i(1-\delta)kz} e^{-\beta kz} \qquad \mu = 2\beta$$

EM waves scattering by an electron

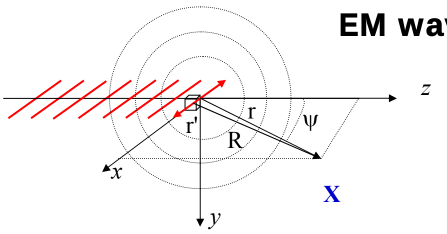

$$\mathbf{E}_{in} = \mathbf{E}_0 e^{-i\omega t},\ \ \mathbf{E}_0 // \hat{\boldsymbol{x}}$$

$$m\mathbf{a} = -e(\mathbf{E}_{in} + \mathbf{v} \times \mathbf{B}_{in})$$

The retarded vector potential $\mathbf{A}(\mathrm{r}, t) = \frac{1}{4\pi\varepsilon_0 c^2}\int_V \frac{\mathbf{J}(\mathrm{r}', t')}{|\mathrm{r} - \mathrm{r}'|} d\mathrm{r}' \quad t' = t - |\mathrm{r} - \mathrm{r}'|/c$

<u>Far away from the electron:</u>

The dipole approximation $|\mathbf{r} - \mathbf{r}'| \approx r \quad \mathbf{A}(\mathrm{r}, t) \approx \frac{1}{4\pi\varepsilon_0 c^2 r}\int_V \mathbf{J}(\mathrm{r}', t - r/c) d\mathrm{r}'$

$$\mathbf{E} = -\nabla\Phi - \frac{\partial \mathbf{A}}{\partial t}$$

$$\frac{\mathbf{E}(\mathrm{t})}{\mathbf{E}_{in}(\mathrm{t})} = -r_0 \frac{e^{i\mathbf{k}\cdot\mathbf{r}}}{r} \cos\psi$$

The scattering involves a phase shift of π

Thomson scattering length (the classical electron radius)

$$r_0 = \frac{e^2}{4\pi\varepsilon_0 mc^2} = 2.82 \times 10^{-5}\,\text{Å}$$

$$\frac{d\sigma}{d\Omega} = r_0^2 \cos^2\psi$$

$$\sigma_T = r_0^2 \int \cos^2\psi\, d\Omega = \frac{8\pi}{3} r_0^2$$

X-rays scattered by an atom

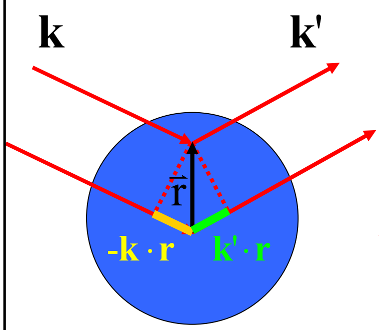

$e^{i\mathbf{q}\cdot\mathbf{r}}$

Momentum transfer (in units of $\hbar$)

$$\mathbf{q} \equiv \mathbf{k}' - \mathbf{k}$$

elastic scattering $|\mathbf{k}| = |\mathbf{k}'| = k$

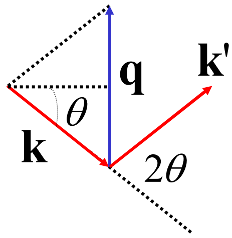

$$|\mathbf{q}|^2 = |\mathbf{k}' - \mathbf{k}|^2$$
$$q^2 = k^2 - 2kk'\cos 2\theta + k^2$$
$$= 2k^2(1 - \cos 2\theta)$$
$$= 4k^2 \sin^2\theta$$
$$q = 2k\sin\theta$$

A volume element $d^3\mathrm{r}$ at $\mathbf{r}$ will contribute an amount $-r_0\rho(\mathbf{r})d^3\mathrm{r}$ to the scattered field with a phase factor $e^{i\mathbf{q}\cdot\mathbf{r}}$.

7

X-rays scattering

Scattering amplitude: $-r_0\int \rho(\vec{r})e^{i\vec{q}\cdot\vec{r}}d\vec{r} = -r_0 f^0(\vec{q})$

Atomic scattering factor $f^0(\vec{q}) \equiv \int \rho(\vec{r})e^{i\vec{q}\cdot\vec{r}}d\vec{r}$

$q \to 0,\quad f^0(\vec{q}) = Z$ (the number of electrons in the atom)

All of the different volume elements scatter in phase; each electron contributes $-r_0$ to the scattered field.

f^0 is independent on photon energy $\hbar\omega$; it is the scattering amplitude in units of $-r_0$.

f^0 is the Fourier transform of the charge distribution.

Optical theorem

absorption cross-section

$$\sigma = -\frac{4\pi r_0}{k} f'' = -\frac{4\pi}{k}\mathrm{Im}(f)$$

8

How does the scattering amplitude *f* change if the photon energy approaches an absorption edge?

The forced charge oscillator: a classical model of an electron bound in an atom.

$$m\ddot{\mathbf{x}} = -e\mathbf{E} - \kappa\mathbf{x} - \Gamma'\dot{\mathbf{x}}$$ damping force

$$\ddot{x} + \Gamma\dot{x} + \omega_s^2 x = -\frac{e\mathrm{E}_0}{m}\mathrm{e}^{-i\omega t} \qquad \omega_s \equiv \sqrt{\kappa/m}, \quad \Gamma \equiv \Gamma'/m$$

$$x = x_0\mathrm{e}^{-i\omega t}, \quad x_0 = -\frac{eE_0}{m}\frac{1}{(\omega_s^2 - \omega^2 - i\omega\Gamma)}$$

$$\mathbf{E}_{sca}(r,t) = -r_0\frac{\omega^2}{(\omega^2 - \omega_s^2 + i\omega\Gamma)}\frac{\mathrm{e}^{ikr}}{r}\mathbf{E}_{in}$$

Resonant scattering amplitude in units of $-r_0$:

$$f_s = \frac{\omega^2}{(\omega^2 - \omega_s^2 + i\omega\Gamma)}$$

9

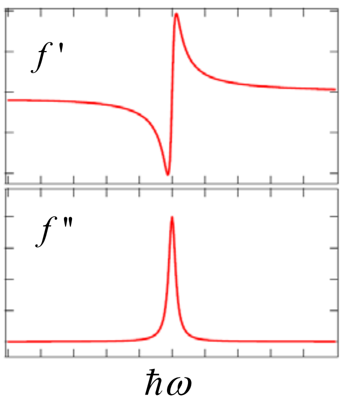

$$f = f' + i f''$$

$$f' = \frac{\omega_s^2(\omega^2 - \omega_s^2)}{(\omega^2 - \omega_s^2)^2 + (\omega\Gamma)^2}$$

$$f'' = -\frac{\omega_s^2\omega\Gamma}{(\omega^2 - \omega_s^2)^2 + (\omega\Gamma)^2}$$

Absorption

$$\sigma = -\frac{4\pi}{k}\mathrm{Im}(f)$$

Resonant scattering

As the photon energy $\hbar\omega$ approaches the binding energy of one of the core-level electrons,

$$f_s(\mathbf{q},\hbar\omega) = f^0(\mathbf{q}) + \underbrace{f'(\hbar\omega) + i f''(\hbar\omega)}_{\text{dispersion corrections}}$$

10

Soft X-ray Absorption and Resonant Scattering

1. Basics of x-ray scattering and absorption
2. **Soft X-ray Absorption**
   - Experimental Setup
   - Applications
     - Chemical analysis
     - Orbital polarization
     - Magnetic Circular Dichroisn
3. Resonant Soft X-ray Scattering
   - Basics
   - Examples
     - Verwey transition of Fe_3O_4
     - Charge-Orbital ordering and Quasi-2D magnetic ordering of $La_{0.5}Sr_{1.5}MnO_4$

11

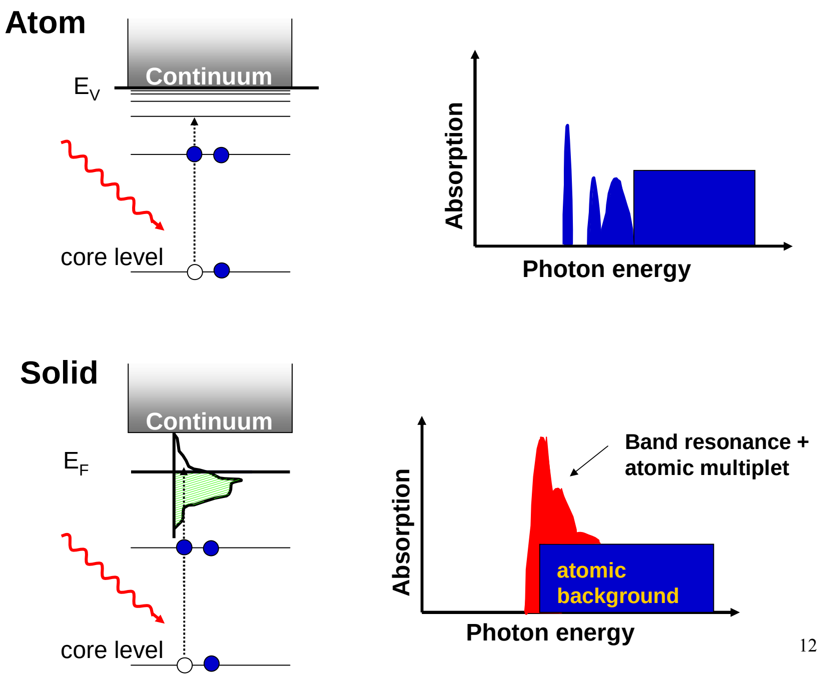

12

Photo-absorption $\frac{d\sigma}{d\Omega} \propto \sum \left| \left\langle \Psi_f \middle| \mathbf{A} \cdot \mathbf{P} \middle| \Psi_i \right\rangle \right|^2 \cdot \delta\left(E_f - E_i - h\nu\right)$

If $\mathbf{k} \cdot \mathbf{r} \ll 1$, **Dipole approximation:** $e^{i\mathbf{k}\cdot\mathbf{r}} \approx 1 + i\mathbf{k}\cdot\mathbf{r} \approx 1$

$$\mathbf{A} = \boldsymbol{\varepsilon} e^{i(\mathbf{k}\cdot\mathbf{r} - \omega t)} \approx \boldsymbol{\varepsilon} e^{-i\omega t}$$

polarization of x-ray

$$\frac{d\sigma}{d\Omega} \propto \sum \left| \left\langle f \middle| \boldsymbol{\varepsilon} \cdot \mathbf{P} \middle| i \right\rangle \right|^2 \cdot \delta\left(E_f - E_i - h\nu\right) \propto \sum \left| \left\langle f \middle| \boldsymbol{\varepsilon} \cdot \mathbf{r} \middle| i \right\rangle \right|^2 \cdot \delta\left(E_f - E_i - h\nu\right)$$

$$\because \langle f | \boldsymbol{\varepsilon} \cdot \mathbf{P} | i \rangle \approx \frac{im}{\hbar} \boldsymbol{\varepsilon} \cdot \langle f | [\hat{H}, \mathbf{r}] | i \rangle = \frac{im}{\hbar}(E_f - E_i) \boldsymbol{\varepsilon} \cdot \langle f | \mathbf{r} | i \rangle = im\omega \langle f | \boldsymbol{\varepsilon} \cdot \mathbf{r} | i \rangle$$

$$[\hat{H}, \mathbf{r}] = \frac{\hbar}{i} \frac{\mathbf{P}}{m}, \quad \text{if } [V(r), \mathbf{r}] = 0$$

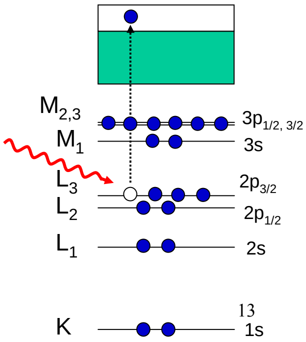

$1s \rightarrow np$ K-edge XAS can be accurately described with single-particle methods.

$2p \rightarrow 3d$ L-edge XAS: the single-particle approximation breaks down and the pre-edge structure is affected by the core hole wave function. The multiplet effect exists.

13

Dipole transition

Absorption probability: $W = \frac{2\pi}{\hbar} \left| M_{ij} \right|^2 \delta(\hbar\omega - E_f + E_i)$ $\quad M_{ij} \propto \left\langle f \middle| \boldsymbol{\varepsilon} \cdot \hat{\mathbf{r}} \middle| i \right\rangle$

$$\boldsymbol{\varepsilon} \cdot \hat{\mathrm{r}} = e_x \sin\theta \cos\phi + e_y \sin\theta \sin\phi + e_z \cos\theta$$

$$\hat{\mathrm{r}} = (\sin\theta\cos\phi, \sin\theta\sin\phi, \cos\theta)$$

$$\cos\theta = \sqrt{\tfrac{4\pi}{3}} Y_{1,0}(\theta,\phi) \qquad \sin\theta \cdot e^{\pm i\phi} = \mp\sqrt{\tfrac{8\pi}{3}} Y_{1,\pm1}(\theta,\phi)$$

$$\boldsymbol{\varepsilon} \cdot \hat{\mathrm{r}} = \sqrt{\tfrac{4\pi}{3}} \left(\frac{-\varepsilon_x + i\varepsilon_y}{\sqrt{2}} Y_{1,1} + \frac{\varepsilon_x + i\varepsilon_y}{\sqrt{2}} Y_{1,-1} + \varepsilon_z Y_{1,0} \right)$$

Selection rule: $(\Delta m_l \equiv m_f - m_i)$ $\quad \Delta m_l = 0$

$$\Delta l \equiv l_f - l_i = \pm 1$$

L. circularly polarized $\quad$ **R. circularly polarized**

$Y_{1,1}$: $\Delta m_l = +1$ $\quad$ $Y_{1,-1}$: $\Delta m_l = -1$

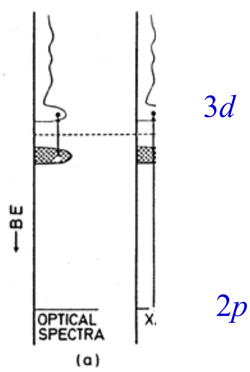

For 2p → 3d: $M_{ij} \propto \left\langle 2p^5 3d^{n+1} \middle| \boldsymbol{\varepsilon} \cdot \mathbf{r} \middle| 2p^6 3d^n \right\rangle$

14

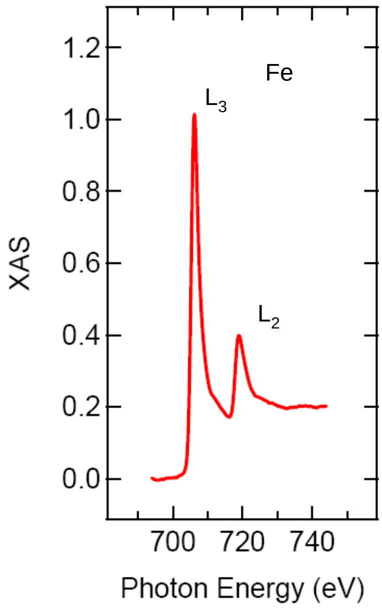

•Two absorption "peaks" from 2p → 3d:

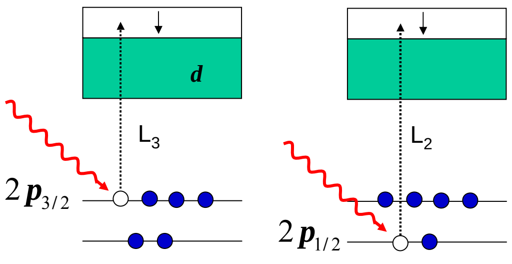

•Absorption cross section is proportional to numbers of d holes and density of states in the core level.

L-edge XAS provides information on the chemical state, orbital symmetry, and spin state of materials.

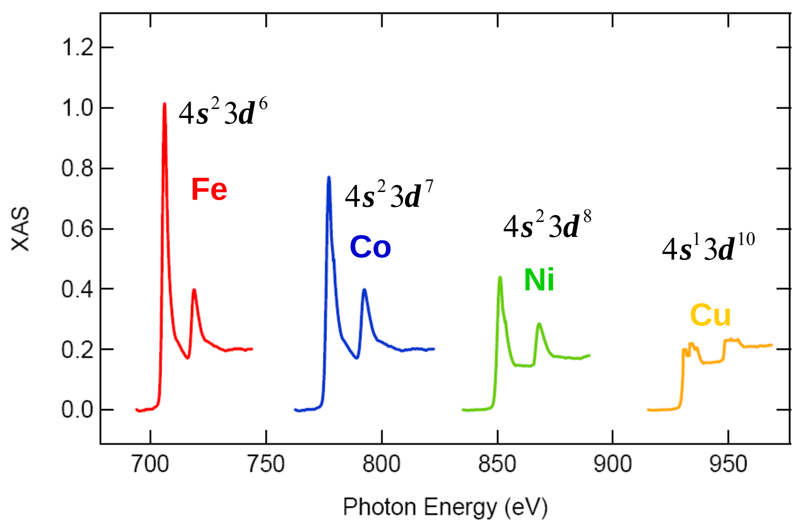

Each element has specific absorption energies.
"finger print" → element specific spectroscopy

Soft X-ray Absorption and Resonant Scattering

1. Basics of x-ray scattering and absorption
2. Soft X-ray Absorption
   - Experimental Setup: how to measure XAS spectra?
   - Applications
     - Chemical analysis
     - Orbital polarization
     - Magnetic Circular Dichroisn
3. Resonant Soft X-ray Scattering
   - Basics
   - Examples
     - Verwey transition of Fe_3O_4
     - Charge-Orbital ordering and Quasi-2D magnetic ordering of $La_{0.5}Sr_{1.5}MnO_4$

17

Measurement of Soft X-ray absorption

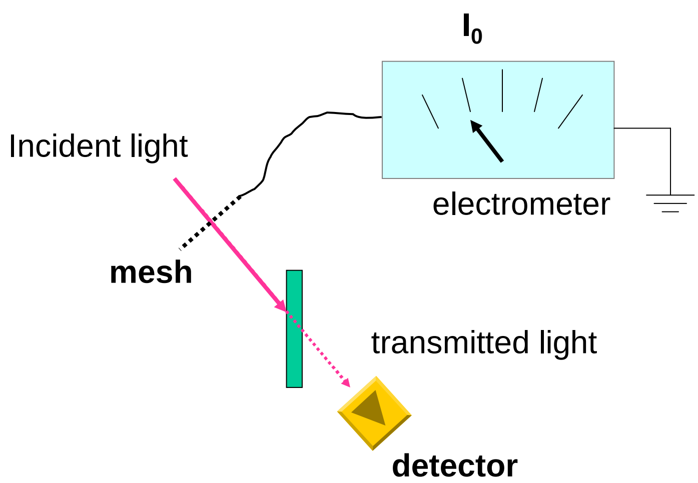

18

Photoexcitation and Relaxation

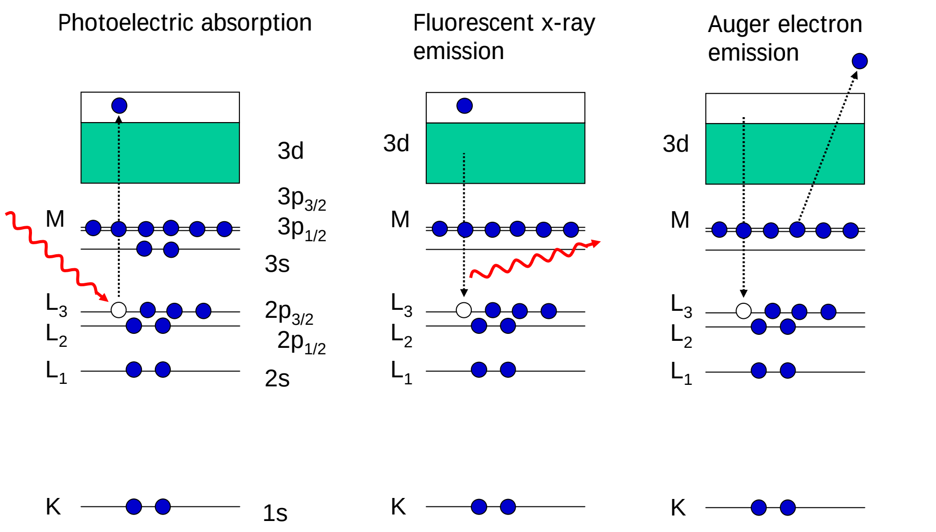

19

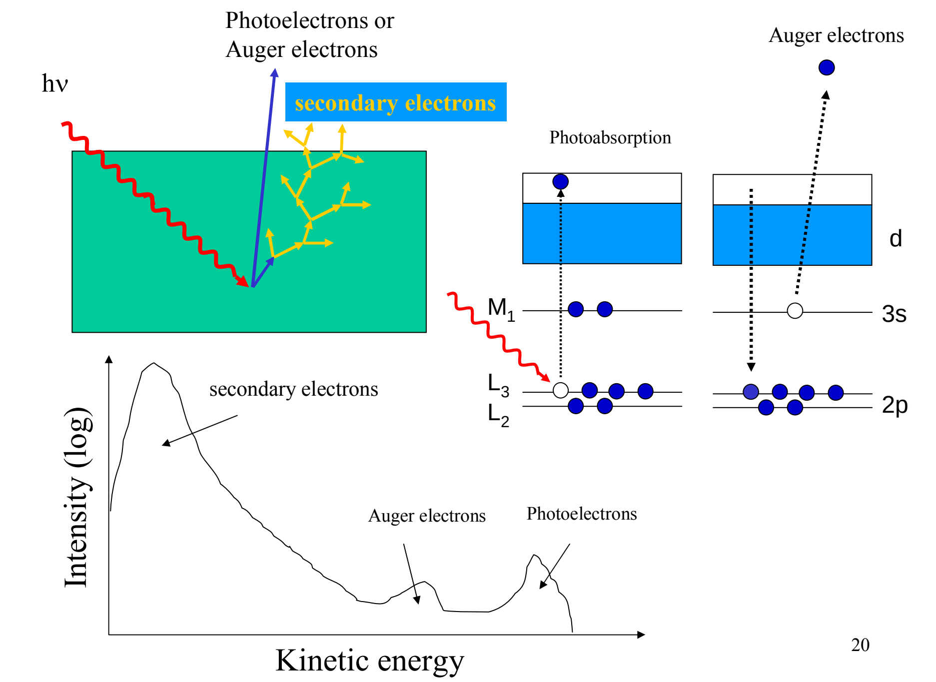

20

Measurement of Soft X-ray absorption

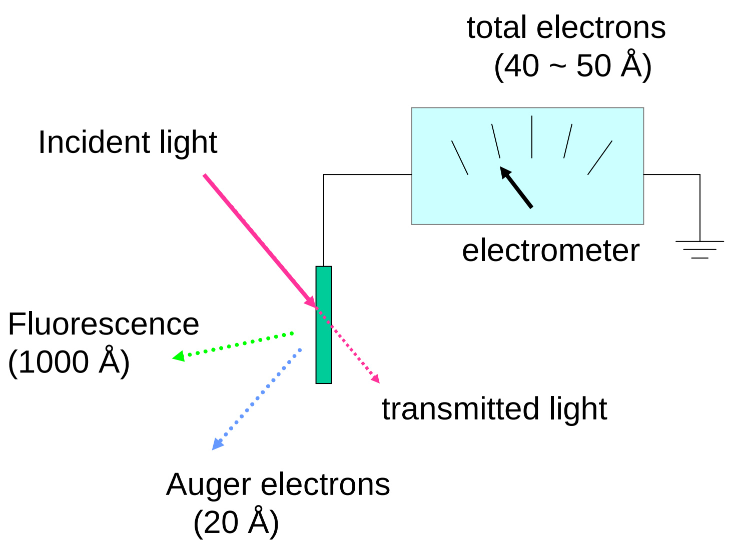

21

Soft X-ray Absorption and Resonant Scattering

1. Basics of x-ray scattering and absorption
2. Soft X-ray Absorption
    - Experimental Setup
    - Applications
        - \- Chemical analysis
        - \- Orbital polarization
        - \- Magnetic Circular Dichroisn
3. Resonant Soft X-ray Scattering
    - Basics
    - Examples
        - \- Verwey transition of Fe_3O_4
        - \- Charge-Orbital ordering and Quasi-2D magnetic ordering of $La_{0.5}Sr_{1.5}MnO_4$

22

In transition-metal oxides

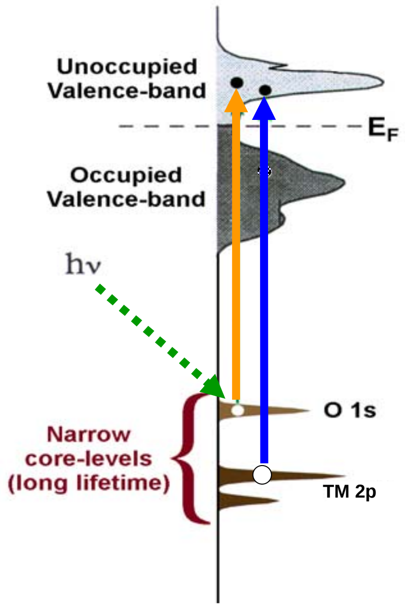

soft x-ray absorption & scattering

TM: 2p → 3d
O: 1s → 2p

direct, element-specific probing of electronic structure of TMO

23

L-edge XAS provides information on the chemical state, orbital symmetry, and spin state of materials.

24

hole doping: $Mn^{3+} \rightarrow Mn^{4+}$

$LaMnO_3$ → $La_{1-x}Sr_xMnO_3$

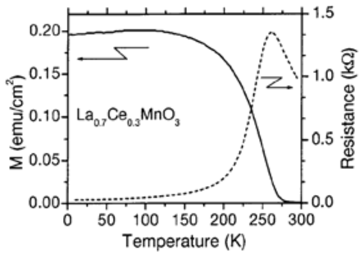

$La_{0.7}Ce_{0.3}MnO_3$ ***electron doping?*** $Mn^{3+} \rightarrow Mn^{2+}$

Mn

$4s^2 3\boldsymbol{d}^5$

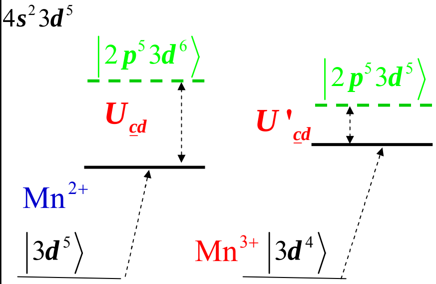

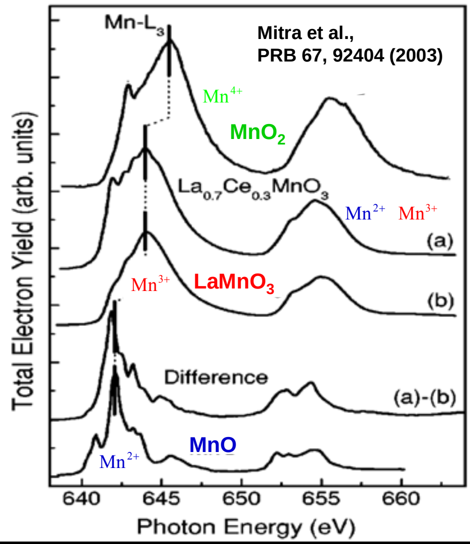

- **Coulomb interactions of 3*d***
- **Interaction between core hole and valence states**

L-edge XAS provides information on the chemical state, orbital symmetry, and spin state of materials.

26

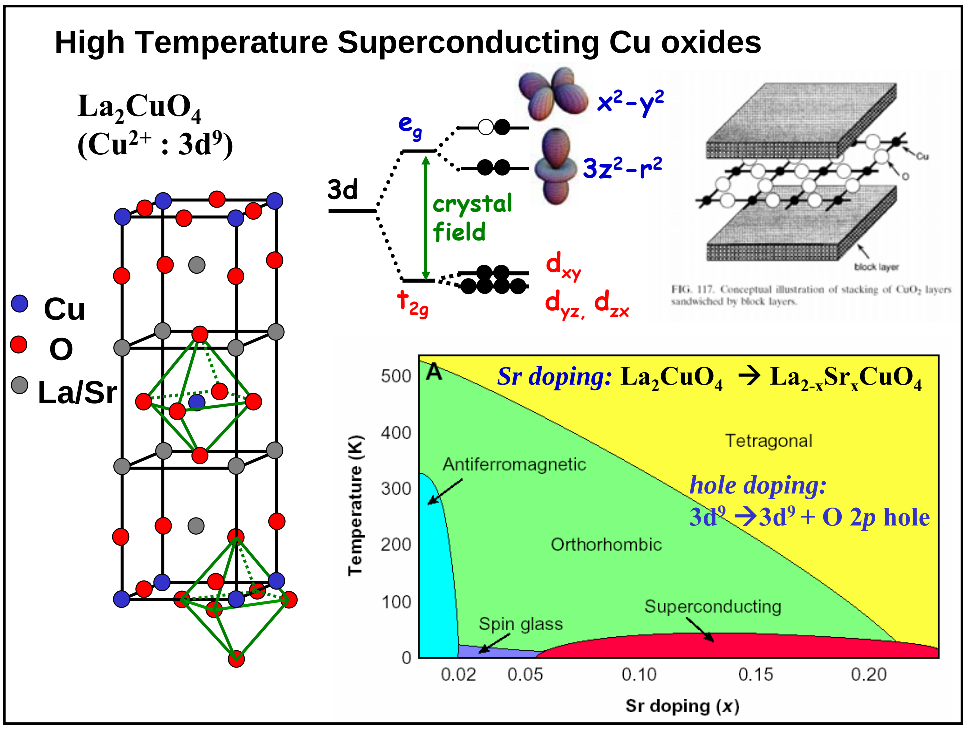
High Temperature Superconducting Cu oxides
La2CuO4
(Cu2+ : 3d9)
Cu
O
La/Sr
3d
eg
t2g
crystal field
x2-y2
3z2-r2
dxy
dyz, dzx
FIG. 117. Conceptual illustration of stacking of CuO2 layers sandwiched by block layers.
block layer
Cu
O
A
Sr doping: La2CuO4 → La2-xSrxCuO4
Tetragonal
Antiferromagnetic
hole doping:
3d9 → 3d9 + O 2p hole
Orthorhombic
Superconducting
Spin glass
Temperature (K)
500
400
300
200
100
0
0.02
0.05
0.10
0.15
0.20
Sr doping (x)

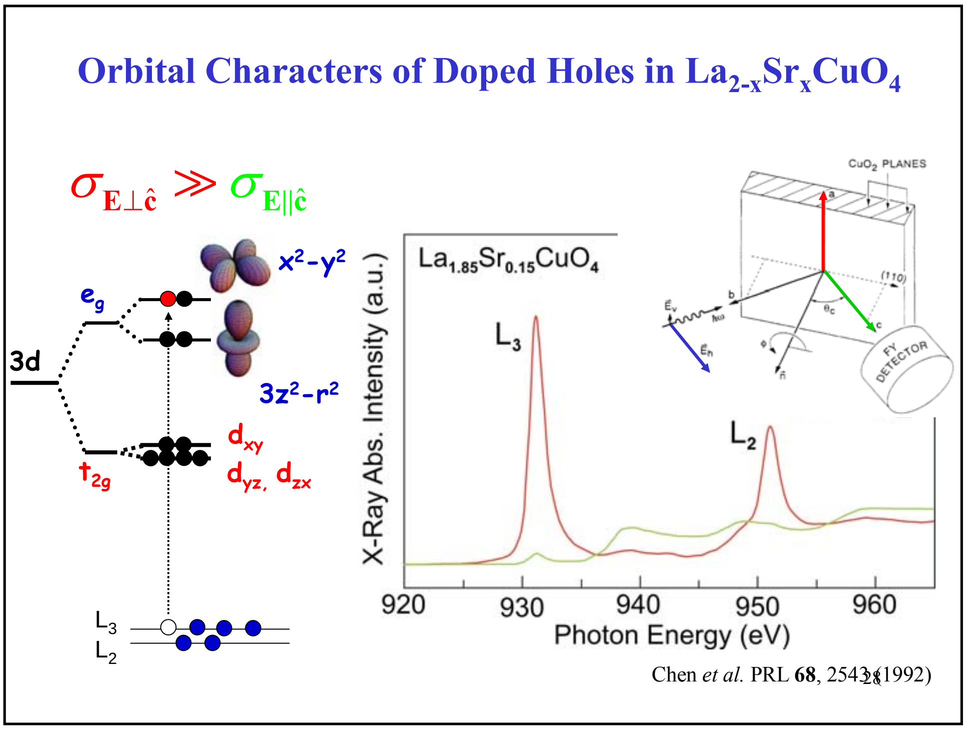
Orbital Characters of Doped Holes in La2-xSrxCuO4
σE⊥ĉ ≫ σE||ĉ
3d
eg
t2g
x2-y2
3z2-r2
dxy
dyz, dzx
L3
L2
La1.85Sr0.15CuO4
L3
L2
X-Ray Abs. Intensity (a.u.)
920
930
940
950
960
Photon Energy (eV)
CuO2 PLANES
FY DETECTOR
Chen et al. PRL 68, 2543 (1992)
28

O 1s X-Ray Absorption on TMO

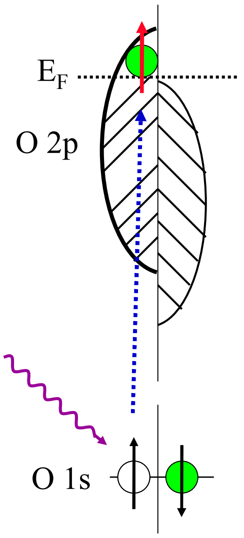

In a cluster appro

O 1s XAS

$$|\Phi\rangle = \alpha' \underbrace{|d^{n+1}\rangle}_{d^{10}} + \cdots$$

$$|d^n\rangle \rightarrow |d^{n+1}\rangle$$

(neglecting 1s core hole)

A: $d^9\underline{L} \rightarrow d^9$

spectral weight arising from doped holes

($\alpha^2 << \beta^2$)

B: $d^9 \rightarrow d^{10}$

upper Hubbard band

Spectral weight transfer: a fingerprint of strong electron correlations

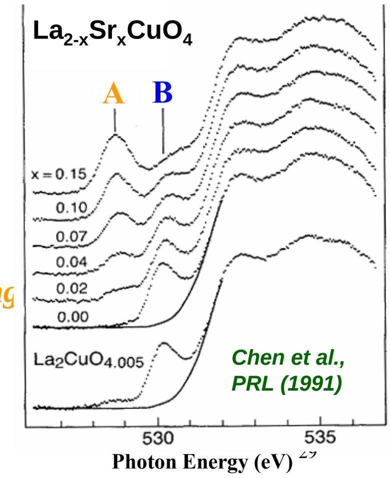

Soft X-ray Absorption and Resonant Scattering

1. Basics of x-ray scattering and absorption
2. Soft X-ray Absorption
   - Experimental Setup
   - Applications
     - Chemical analysis
     - Orbital polarization
     - Magnetic Circular Dichroisn
3. Resonant Soft X-ray Scattering
   - Basics
   - Examples
     - Verwey transition of Fe_3O_4
     - Charge-Orbital ordering and Quasi-2D magnetic ordering of $La_{0.5}Sr_{1.5}MnO_4$

30

Magnetic materials:

In some solids, individual ions have non vanishing average vector moments below a critical temperature. Such solids are called *magnetically ordered*.

If a solid exhibits a spontaneous magnetization, its ordered state is described as *ferromagnetic* or *ferrimagnetic*. A solid with magnetic ordering has no spontaneous called antiferromagnetic.

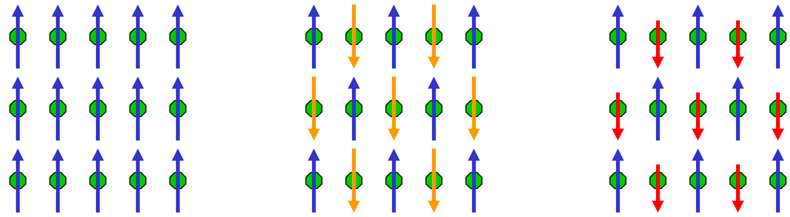

ferromagnetism (FM) anti-ferromagnetism (AFM) ferrimagnetism

31

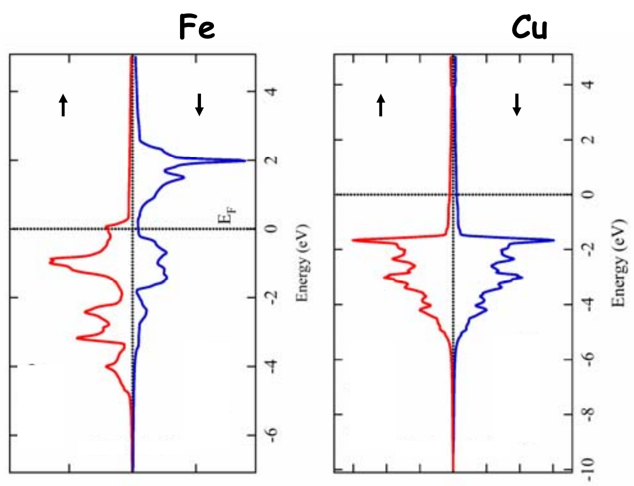

Density of states Density of states

32

Polarization of Synchrotron Radiation

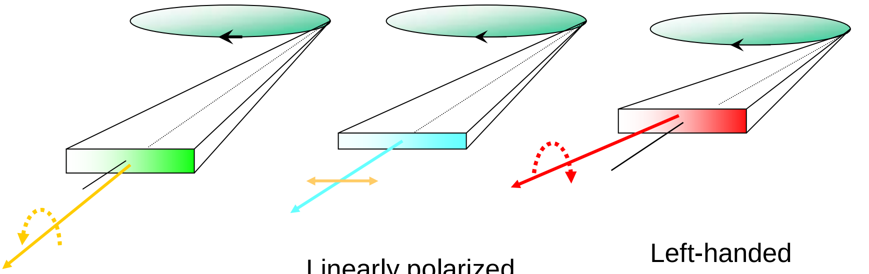

Linearly polarized

Left-handed
circularly polarized

Right-handed
circularly polarized

33

Soft X-Ray Magnetic Circular Dichroism in Absorption

For $2p_{3/2} \rightarrow 3d$

Right-handed circularly polarized light preferentially excites spin-down electrons.

Left-handed circularly polarized light preferentially excites spin-up electrons.

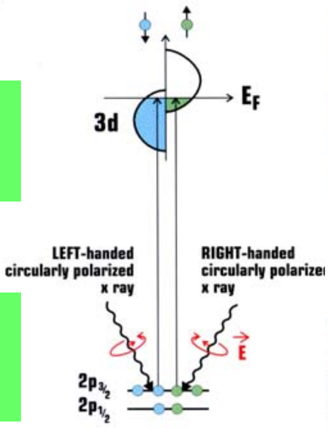

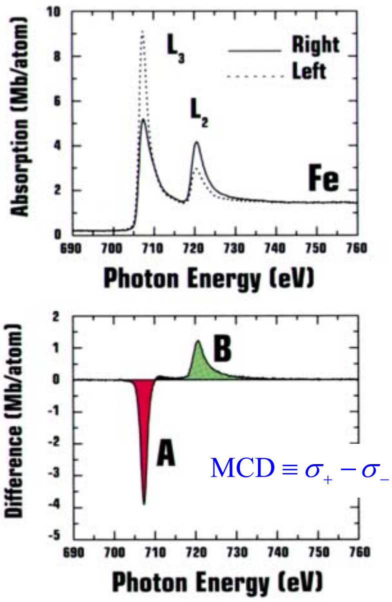

MCD is defined as the difference in absorption intensity of magnetic systems excited by left and right circularly polarized light.

MCD sum rules

$$m_{orb} = -\frac{4\int_{L_3+L_2}(\mu_+ - \mu_-)d\omega}{3\int_{L_3+L_2}(\mu_+ + \mu_-)d\omega}\times(10-n_{3d})$$

$$m_{spin} = -\frac{6\int_{L_3}(\mu_+ - \mu_-)d\omega - 4\int_{L_3+L_2}(\mu_+ - \mu_-)d\omega}{\int_{L_3+L_2}(\mu_+ + \mu_-)d\omega}\times(10-n_{3d})\times\left(1+\frac{7\langle T_z\rangle}{2\langle S_z\rangle}\right)^{-1}$$

— Thole *et al.*, PRL **68**, 1943 (1992)
P. Carra *et al.*, PRL **70**, 694 (1993)

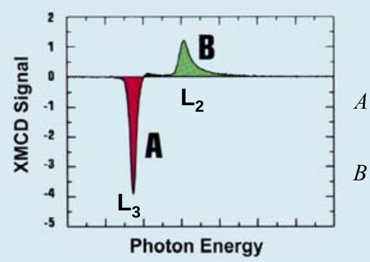

$A \equiv \int_{L_3}(\mu_+ - \mu_-)$

$B \equiv \int_{L_2}(\mu_+ - \mu_-)$

- **Orbital Magnetic Moment**
  $m_{orb} \propto (A+B)$
- **Spin Magnetic Moment**
  $m_{spin} + m_D \propto (A-2B)$

Experimental confirmation:
Chen et al., PRL 75, 152 (1995)

35

Soft X-Ray Magnetic Circular Dichroism in Absorption

Soft X-ray MCD in absorption provides
a unique means to probe:

element-specific magnetic hysteresis
orbital and spin moments
magnetic coupling.

There are two ways to obtain a MCD spectrum:
1) **Fixing M, measure XAS with left and right circular lights.**
2) **Fixing the helicity of light, measure XAS with two opposite directions of M.**

36

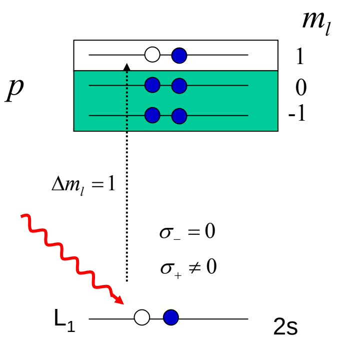

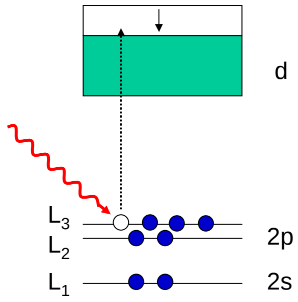

$s \rightarrow p$

MCD in K-edge or L_1-edge XAS is not sensitive to spin magnetic moments. Instead, the MCD measures orbital moments.
(H. W.)

$p \rightarrow d$

MCD in L-edge XAS measures both spin and orbital magnetic moments because of the spin-orbit interaction in the core levels.

37

Element-Specific Magnetic Hysteresis Measurements

A New Technique for Studying Interlayer Magnetic Coupling

Chen et al.,
PRB 48, 642 (1993)

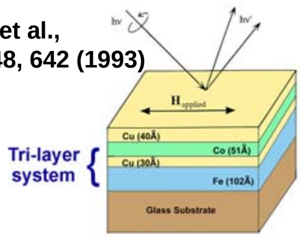

SXMCD Hysteresis Curves

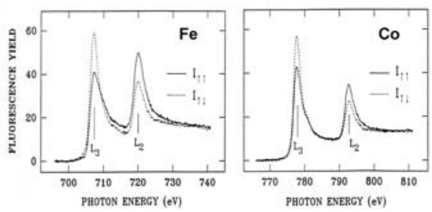

Conventional Hysteresis Curve

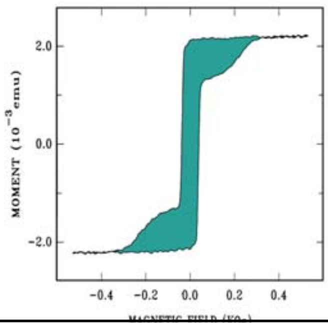

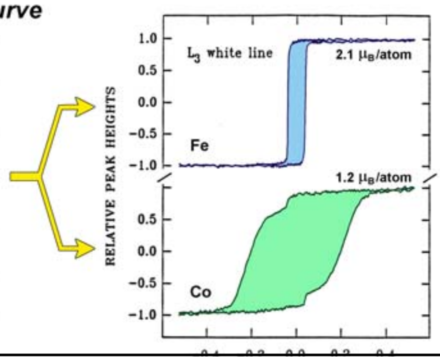

Ferromagnetism in one-dimensional monatomic metal chains

P. Gambardella*, A. Dallmeyer†, K. Maiti†, M. C. Malagoli†, W. Eberhardt†‡, K. Kern*§ & C. Carbone†||

Nature 416, 301 (2001)

Two-dimensional systems, such as ultrathin epitaxial films and superlattices, display magnetic properties distinct from bulk materials[1]. A challenging aim of current research in magnetism is to explore structures of still lower dimensionality[2–6]. As the dimensionality of a physical system is reduced, magnetic ordering tends to decrease as fluctuations become relatively more important[7]. Spin lattice models predict that an infinite one-dimensional linear chain with short-range magnetic interactions spontaneously breaks up into segments with different orientation of the magnetization, thereby prohibiting long-range ferromagnetic order at a finite temperature[7–9]. These models, however, do not take into account kinetic barriers to reaching equilibrium or interactions with the substrates that support the one-dimensional nanostructures. Here we demonstrate the existence of both short- and long-range ferromagnetic order for one-dimensional monatomic chains of Co constructed on a Pt substrate. We find evidence that the monatomic chains consist of thermally fluctuating segments of ferromagnetically coupled atoms which, below a threshold temperature, evolve into a ferromagnetic long-range-ordered state owing to the presence of anisotropy barriers. The Co chains are characterized by large localized orbital moments and correspondingly large magnetic anisotropy energies compared to two-dimensional films and bulk Co.

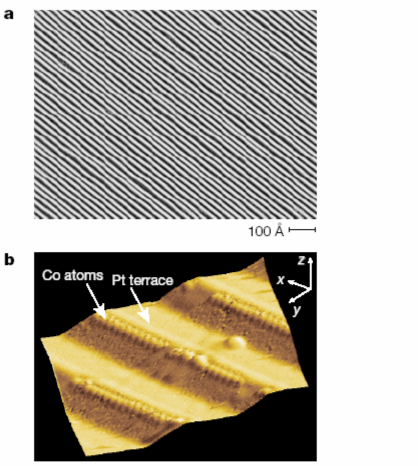

Figure 1 STM topographs of the Pt(997) surface. **a**, Periodic step structure (each white line represents a single step). The surface has a 6.45° miscut angle relative to the (111) direction; repulsive step interactions result in a narrow terrace width distribution centred at 20.2 Å with 2.9 Å standard deviation. **b**, Co monatomic chains decorating the Pt step edges (the vertical dimension is enhanced for better contrast). The monatomic chains are obtained by evaporating 0.13 monolayers of Co onto the substrate held at $T = 260$ K and previously cleaned by ion sputtering and annealing cycles in ultrahigh vacuum (UHV). The chains are linearly aligned and have a spacing equal to the terrace width.

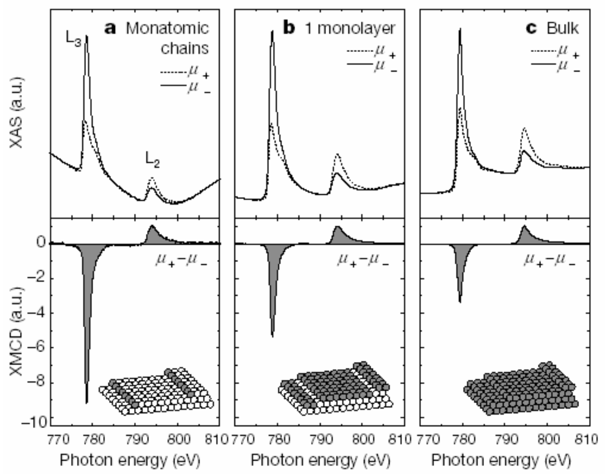

Figure 2 Co X-ray absorption spectra for parallel (μ_+) and antiparallel (μ_-) direction of light polarization and field-induced magnetization. The dichroism signal ($\mu_+ - \mu_-$) is obtained by subtraction of the absorption spectra in each panel and normalization to the L_2 peak. **a**, Monatomic chains; **b**, one monolayer; **c**, thick Co film on Pt(997). The sample was mounted onto a UHV variable-temperature insert that could be rotated with the respect to the direction of the external magnetic field applied parallel to the incident photon beam. Spectra were recorded in the electron-yield mode at $T = 10$ K and

40

Soft X-ray Absorption and Resonant Scattering

1. Basics of x-ray scattering and absorption
2. Soft X-ray Absorption
   - Experimental Setup
   - Applications
     - Chemical analysis
     - Orbital polarization
     - Magnetic Circular Dichroisn
3. Resonant Soft X-ray Scattering
   - Basics
   - Examples
     - Verwey transition of Fe_3O_4
     - Charge-Orbital ordering and Quasi-2D magnetic ordering of $La_{0.5}Sr_{1.5}MnO_4$

41

Correlated-Electron Materials

- Variety of fascinating macroscopic phenomena
- Tunable electronic and magnetic properties

HTSC MIT CMR

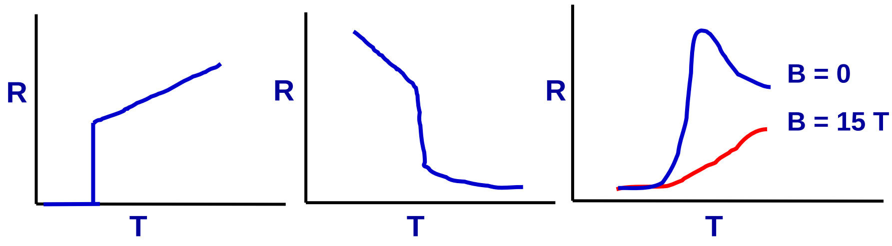

High Temperature SuperConductivity

Metal-to-Insulator Transition

Colossal Magneto-Resistance

42

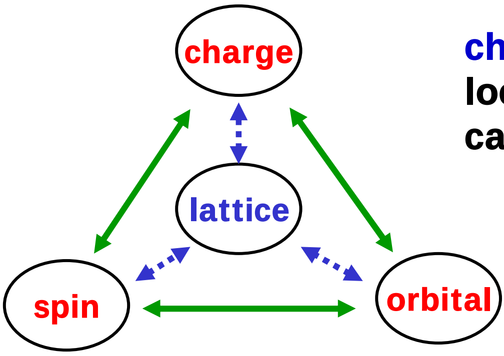

charge ordering: spatial localization of the charge carriers on certain sites

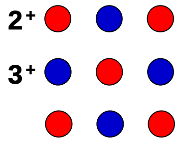

orbital ordering: periodic arrangement of specific electron orbitals

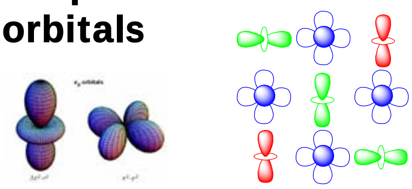

spin ordering: long range ordering of local magnetic moments

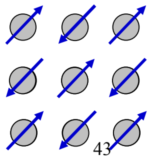

43

Charge-orbital ordering in correlated electron systems

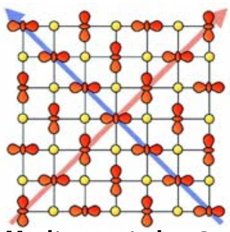

$La_{0.5}Sr_{1.5}MnO_4$

Murakami et al. (1998)

Moritomo et al. (1995)

Sternlieb et al. (1996)

$La_{1/3}Ca_{2/3}MnO_3$

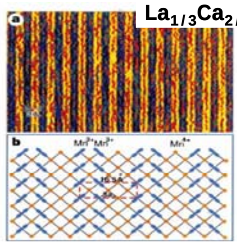

C. H. Chen et al. (1998)

$La_{1.6-x}Nd_{0.4}Sr_xCuO_4$

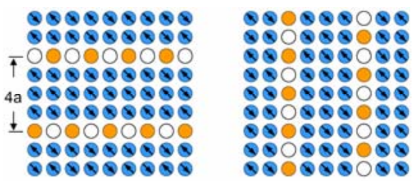

J. Tranquda et al. (1995)

Small valence disproportionation !

$\Delta q / q_{total} << 1$

44

Advantage of Resonant Soft X-ray Scattering

$$f_{res} \sim \sum_{3d} \frac{\langle \Psi_{2p} | \vec{\varepsilon} \cdot \vec{r} e^{i\vec{k}' \cdot \vec{r}} | \Psi_{3d} \rangle \langle \Psi_{3d} | \vec{\varepsilon}_0 \cdot \vec{r} e^{i\vec{k} \cdot \vec{r}} | \Psi_{2p} \rangle}{\hbar\omega - (E_{3d} - E_{2p} - i\Gamma)}$$

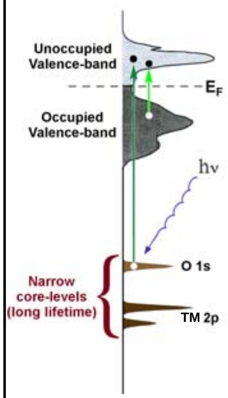

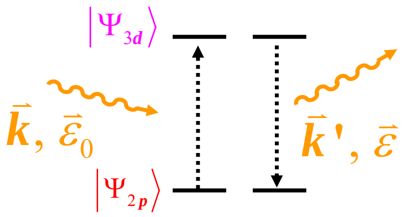

momentum transfer

$$\vec{q} \equiv \vec{k}' - \vec{k}$$

→ **modulation vector**

- **With $\hbar\omega = E_{3d} - E_{2p}$, f_{res} enhanced dramatically and ordering of Ψ_{3d} focused.**

Elastic x-ray scattering

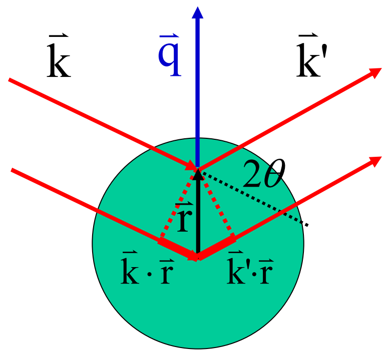

elastic scattering $|\vec{k}| = |\vec{k}'|$

momentum transfer

$$\hbar\vec{q} = \hbar\vec{k}' - \hbar\vec{k}$$

$$q = 2k \sin\theta = \frac{4\pi}{\lambda} \sin\theta$$

A volume element $d^3\vec{r}$ at $\vec{r}$ will contribute an amount to the scattering field with a phase factor $e^{i\vec{q}\cdot\vec{r}}$.

scattering form factor

$$S_q \equiv \sum_j S(\vec{r}_j) e^{i\vec{q}\cdot\vec{r}_j}$$

Fourier transform of spin distribution.

$$\frac{d\sigma}{d\Omega} \propto |S_q|^2$$

Bragg condition:
***q* = modulation vector of charge, spin , or orbital order**

46

X-ray magnetic scattering

$$H_{\text{int}} = \underbrace{\frac{e^2}{2mc^2}\sum_j A(r_j)^2 + \frac{e}{mc}\sum_j A\cdot P_j}_{\text{kinetic energy}} \underbrace{- \frac{e\hbar}{2mc}\sum_j s_j \cdot \nabla\times A}_{\text{m·B}} \underbrace{- \frac{e^2\hbar}{2(mc^2)^2}\sum_j s_j\cdot\left(\frac{\partial A}{\partial t}\times A\right)}_{\text{SO}}$$

Non-resonant

$$\sigma \simeq \frac{2\pi}{\hbar}\left|\langle f|H_{\text{int}}|i\rangle\right|^2$$

Blume, J. Appl. Phys. (1985)

$$= \frac{2\pi}{\hbar}\left(\frac{2\pi\hbar c^2}{V\omega}\frac{e^2}{mc^2}\right)^2 \left|\langle f|\sum_j e^{iq\cdot r_j}|i\rangle\, \varepsilon'\cdot\varepsilon - i\frac{\hbar\omega}{mc^2}\langle f|\sum_j e^{iq\cdot r_j} s_j|i\rangle\cdot\varepsilon'\times\varepsilon\right|^2$$

$$\frac{f_{\text{mag}}}{f_{\text{charge}}} \sim \frac{\hbar\omega}{mc^2} \sim 10^{-3} \qquad \frac{\sigma_{\text{mag}}}{\sigma_e} \sim 10^{-6}$$

Resonant

for $\hbar\omega \sim 600$ eV

$$\sigma \simeq \frac{2\pi}{\hbar}\left|\sum_n \frac{\langle f|H_{\text{int}}|n\rangle\langle n|H_{\text{int}}|i\rangle}{E_i + \hbar\omega - E_n}\right|^2 \delta(E_i - E_f)$$

47

Resonant X-ray magnetic scattering

electric dipole transitions

Hannon et al., PRL(1988)

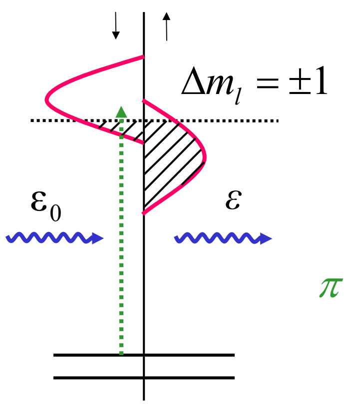

$$f_{mag}^{res} = -i\frac{3\lambda}{8\pi}(\varepsilon^* \times \varepsilon_0)\cdot\hat{z}(F_{1,1} - F_{1,-1})$$

$\Delta m_l = 1$ $\quad$ $\Delta m_l = -1$

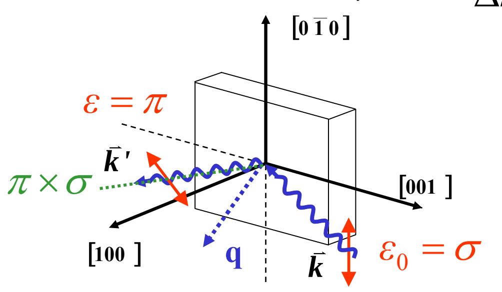

As a result of spin-orbit and exchange interactions, magnetic ordering manifests itself in resonant scattering.

Resonant Soft X-ray Scattering

Charge-orbital ordering in manganite and magnetite

- Wilkins et al., PRL (2003)
- Thomas et al., PRL (2004)
- Dhesi et al., PRL (2004)
- Huang et al., PRL (2006)

....

CDW or charge stripes in cuprate and nickelate

- Abbamonte et al., Nature (2004)
- Abbamonte et al., Nature Physics (2005)
- Schüßler-Langeheine et al., PRL (2005)

......

Antiferromagnetic ordering of manganite

- Wilkins et al., PRL (2003)
- Okamoto et al., PRL(2007)

49

Soft X-ray Absorption and Resonant Scattering

1. Basics of x-ray scattering and absorption
2. Soft X-ray Absorption
   - Experimental Setup
   - Applications
     - Chemical analysis
     - Orbital polarization
     - Magnetic Circular Dichroisn
3. Resonant Soft X-ray Scattering
   - Basics
   - Examples
     - Verwey transition of Fe_3O_4
     - Charge-Orbital ordering and Quasi-2D magnetic ordering AFM of $La_{0.5}Sr_{1.5}MnO_4$

50

The Verwey transition of magnetite (Fe_3O_4)

- **Inverted spinel structure (cubic)**
  - **1/3: tetrahedral (A-site) Fe^{3+}**
  - **2/3: octahedral (B-site) Fe^{3+}, Fe^{2+}**
- **Verwey model:**

charge order-disorder transition of B-site Fe^{3+} & Fe^{2+} with T_V ~ 120 K

Fe_3O_4 is believed to be a classic example of charge ordering.

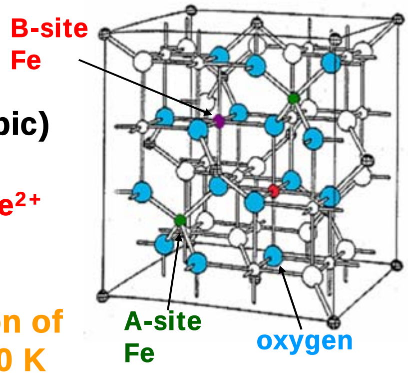

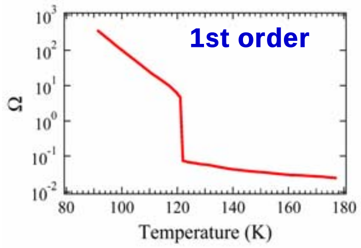

Refinement of x-ray and neutron diffraction

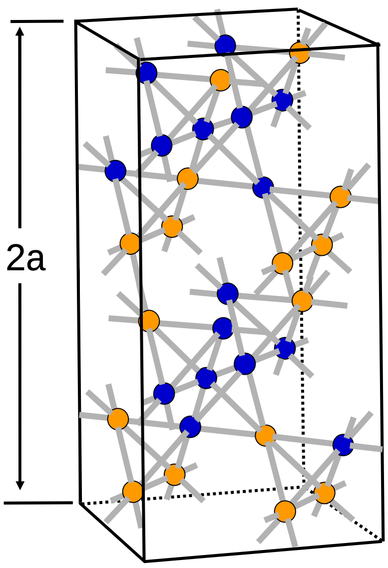

B-site ● Fe^{2+} ● Fe^{3+}

- **Charge ordering deduced from the Fe-O distance.**
- **Valence of B-site Fe: 2.4 & 2.6 (rather than 2 & 3)**
- **$(0\ 0\ 1)_c$ and $(0\ 0\ 1/2)_c$ charge modulation along the c-axis**

Wright, Attfield, and Radaelli, PRL (2001), PRB (2002)

52

LDA+U calculations: charge-orbital ordering

Jeng, Guo, and Huang, PRL (2004)

Leonov et al., PRL (2004)

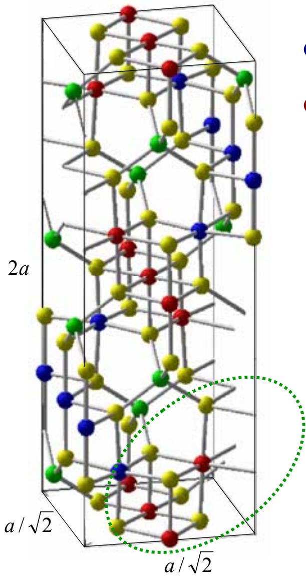

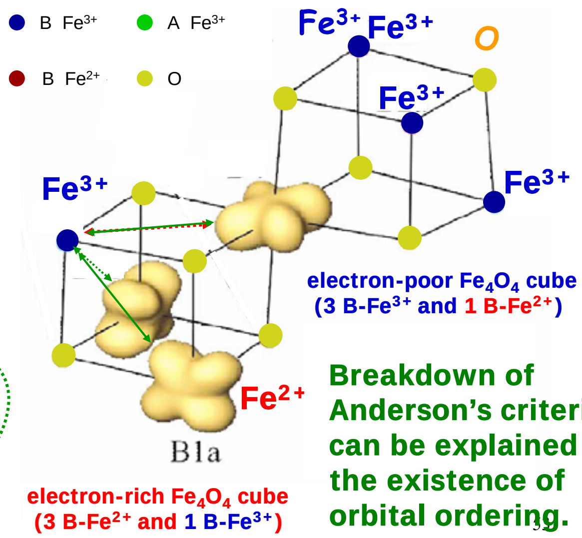

Breakdown of Anderson's criterion can be explained by the existence of orbital ordering.

$(0\ 0\ \frac{1}{2})_c$ resonant scattering at O *K*-edge of Fe_3O_4

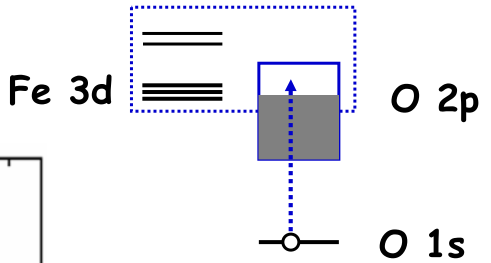

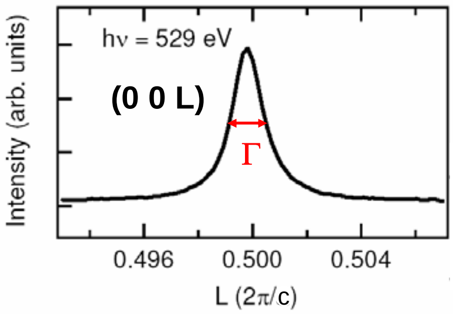

Correlation length $\xi \equiv 1/\Gamma$ = 900 Å

The change in the structure factor with $q = (0\ 0\ \frac{1}{2})_c$ around O K-edge is negligible:

$$\frac{|\sum_j (f_{Fe} e^{i\mathbf{q}\cdot\mathbf{r}_j} + f_O e^{i\mathbf{q}\cdot\mathbf{r}_j})|^2}{|\sum_j (f_{Fe} e^{i\mathbf{q}\cdot\mathbf{r}_j} + R \cdot f_O e^{i\mathbf{q}\cdot\mathbf{r}_j})|^2} \approx 1$$

R is the factor accounting for the enhancement of the form factor due to the **O K-edge resonance.**

$(0\ 0\ \frac{1}{2})_c$ resonant scattering at O *K*-edge of Fe_3O_4

$\xi \sim 900$ Å

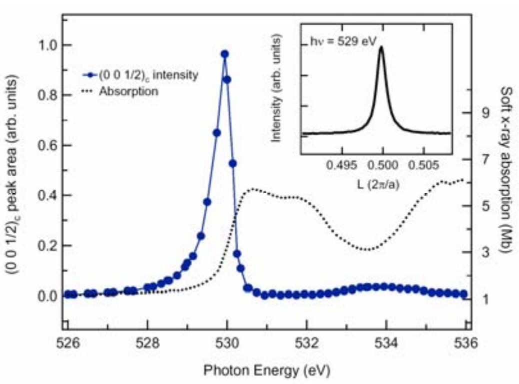

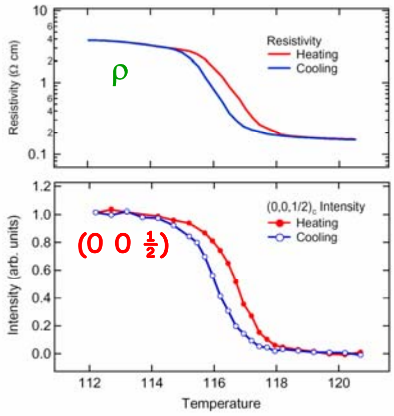

Evidence for the ordering of electronic states associated with the Verwey transition.

Huang et al., PRL (2004)

55

<u>Soft X-ray Absorption and Resonant Scattering</u>

1. Basics of x-ray scattering and absorption
2. Soft X-ray Absorption
   - Experimental Setup
   - Applications
     - Chemical analysis
     - Orbital polarization
     - Magnetic Circular Dichroisn
3. Resonant Soft X-ray Scattering
   - Basics
   - Examples
     - Verwey transition of Fe_3O_4
     - Charge-Orbital ordering and Quasi-2D magnetic ordering of $La_{0.5}Sr_{1.5}MnO_4$

56

Low-dimensional quantum magnetism

Mermin-Wagner (1966): Pure 2D magnetic order only exists at T=0.

2D quantum Heisenberg antiferromagnet on a square lattice with $S = \frac{1}{2}$

spin correlation

$\xi(T) \propto e^{2\pi\rho_S / k_B T}$

Chakravarty et al., PRL 60, 1057 (1988)

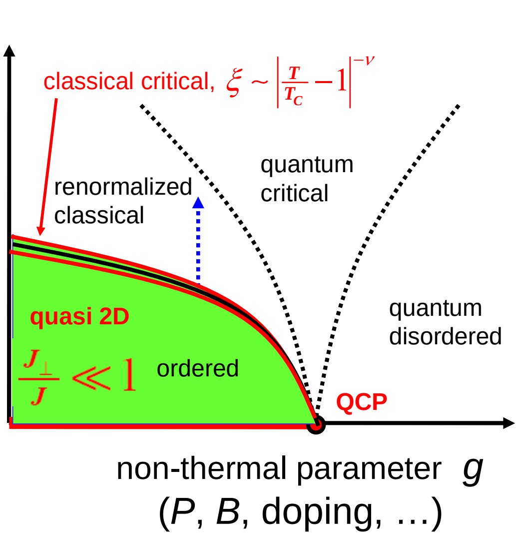

$Sr_2CuO_2Cl_2$

Cu^{2+}, S=1/2, T_N=256 K

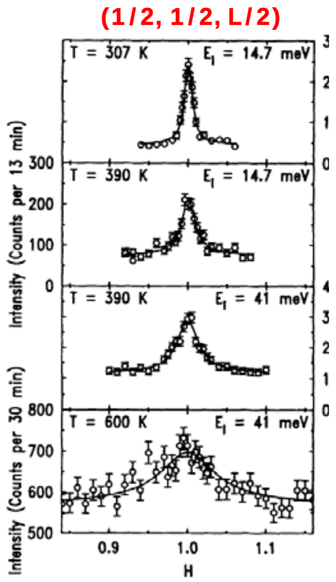

Greven et al., PRL(1994)

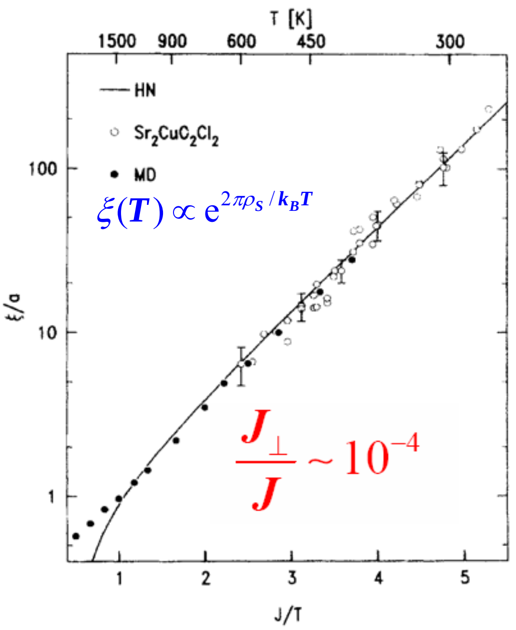

Half-doped single-layered manganite

doping Sr

$LaSrMnO_4 \longrightarrow La_{0.5}Sr_{1.5}MnO_4$

Mn^{3+} (d^4)

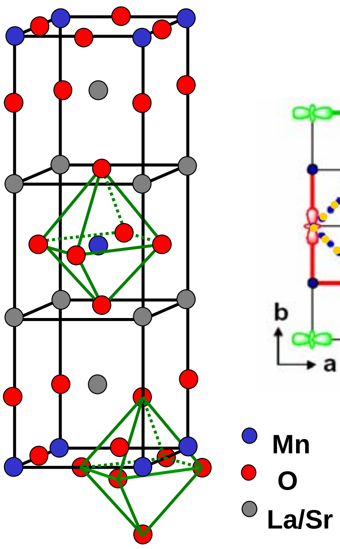

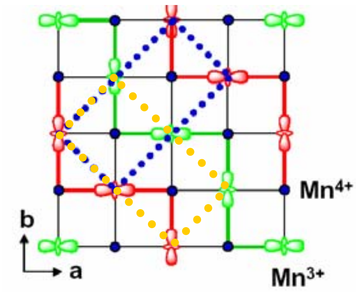

T_N ~ 110 K

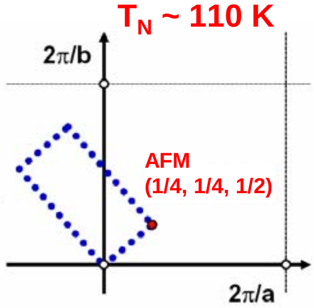

C.O.
(1/4, 1/4, 0)
T_{CO} ~ 220 K

59

Resonant soft x-ray scattering on $La_{0.5}Sr_{1.5}MnO_4$

Mn L-edge (2p→3d)

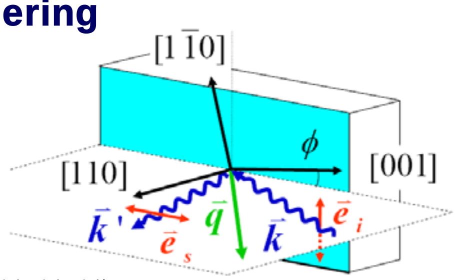

$\phi = 0$

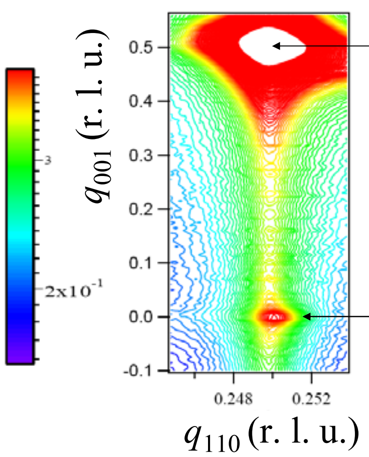

(¼, ¼, ½)
AFM ordering

(¼, ¼, 0)
orbital ordering

$I \propto \cos^2 \phi$

60

$La_{0.5}Sr_{1.5}MnO_4$

113 K (1/4, 1/4, 1/2)

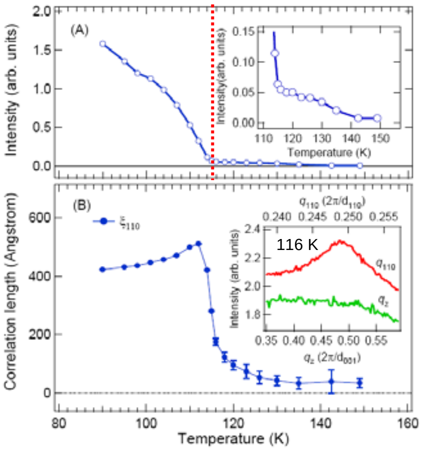

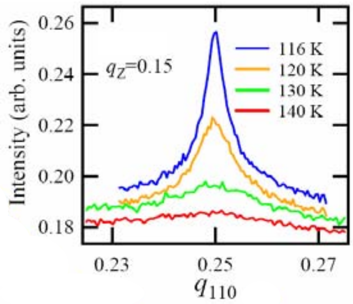

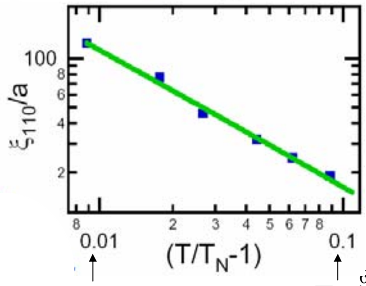

$$\xi \propto \left(\frac{T}{T_N} - 1\right)^{-\nu}, \quad \nu = 0.75 \pm 0.04$$

T=114 K

T=123 K

$La_{0.5}Sr_{1.5}MnO_4$

113 K (1/4, 1/4, 1/2)

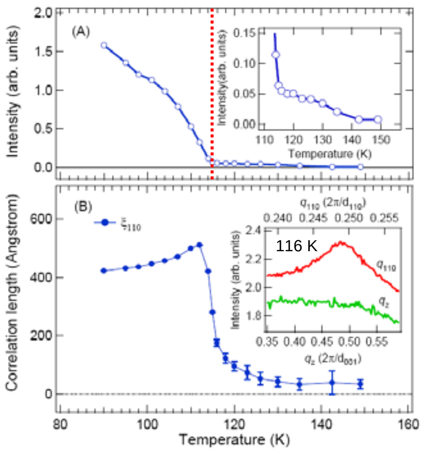

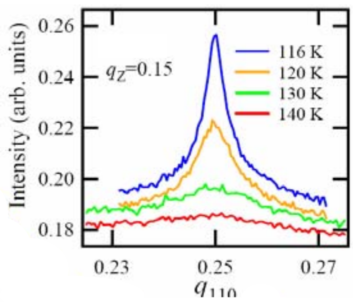

Extension of zero-temperature AFM to T > T_N

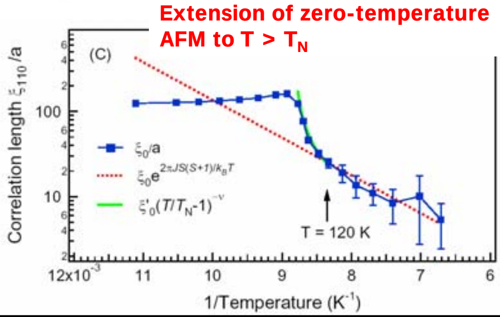

semi- classical

$$\xi(T) \propto e^{2\pi\rho_S/k_BT}$$

Appendix: Basic of Magnetic Circular Dichroism in X-ray Absorption

Considering L-edge $2p_{3/2} \rightarrow 3d$ absorption, and ignoring the spin-orbit interaction in the 3d bands,

$$\sigma \propto \left| \langle l, m_l | \boldsymbol{\varepsilon} \cdot \hat{\mathrm{r}} | j, m_j \rangle \right|^2$$

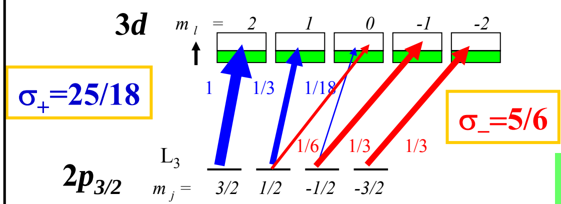

For left-handed circular light

$$\sigma_+ \propto R(r)^2 \cdot \left| \langle Y_{lm} | \frac{\varepsilon_x - i\varepsilon_y}{\sqrt{2}} Y_{1,1} | j, m_j \rangle \right|^2$$

radial part

Left-handed circularly polarized light preferentially excites spin-up electrons.

For light-handed circular light

$$\sigma_- \propto R(r)^2 \cdot \left| \langle Y_{lm} | \frac{\varepsilon_x + i\varepsilon_y}{\sqrt{2}} Y_{1,-1} | j, m_j \rangle \right|^2$$

Right-handed circularly polarized light preferentially excites spin-down electrons.

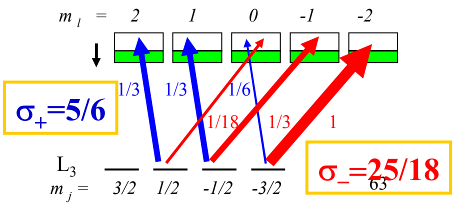

$$\sigma \propto \left| \langle l, m_l | \boldsymbol{\varepsilon} \cdot \hat{\mathrm{r}} | j, m_j \rangle \right|^2$$

$$\hat{\mathrm{r}} = (\sin\theta\cos\phi, \sin\theta\sin\phi, \cos\theta)$$

$$\boldsymbol{\varepsilon} \cdot \hat{\mathrm{r}} = e_x \sin\theta\cos\phi + e_y \sin\theta\sin\phi + e_z \cos\theta$$

$$\cos\theta = \sqrt{\tfrac{4\pi}{3}} Y_{1,0}(\theta,\phi) \quad \sin\theta \cdot e^{\pm i\phi} = \mp\sqrt{\tfrac{8\pi}{3}} Y_{1,\pm 1}(\theta,\phi)$$

$$\boldsymbol{\varepsilon} \cdot \hat{\mathrm{r}} = \sqrt{\tfrac{4\pi}{3}} \left(\tfrac{-\varepsilon_x + i\varepsilon_y}{\sqrt{2}} Y_{1,1} + \tfrac{\varepsilon_x + i\varepsilon_y}{\sqrt{2}} Y_{1,-1} + \varepsilon_z Y_{1,0} \right)$$

$$\sigma_\pm \propto R(r)^2 \cdot \left| \langle Y_{lm} | \frac{\varepsilon_x \mp i\varepsilon_y}{\sqrt{2}} Y_{1,\pm 1} | j, m_j \rangle \right|^2$$

$$\sigma_+ \propto \left| \langle Y_{2,2} | \frac{\varepsilon_x - i\varepsilon_y}{\sqrt{2}} Y_{1,1} | j = \tfrac{3}{2}, m_j = \tfrac{1}{2} \rangle \right|^2 = \tfrac{1}{3}$$

$$\because \langle Y_{2,2} | Y_{1,1} | j = \tfrac{3}{2}, m_j = \tfrac{1}{2} \rangle = \sqrt{\tfrac{1}{3}} \langle Y_{2,2} | Y_{1,1} | Y_{1,1} \rangle = \sqrt{\tfrac{1}{3}}$$

$$\sigma_- \propto \left| \langle Y_{2,0} | \frac{\varepsilon_x + i\varepsilon_y}{\sqrt{2}} Y_{1,-1} | j = \tfrac{3}{2}, m_j = \tfrac{1}{2} \rangle \right|^2 = \tfrac{1}{18}$$

$$\because \langle Y_{2,0} | Y_{1,-1} | j = \tfrac{3}{2}, m_j = \tfrac{1}{2} \rangle = \sqrt{\tfrac{1}{3}} \langle Y_{2,0} | Y_{1,-1} | Y_{1,1} \rangle = \sqrt{\tfrac{1}{18}}$$

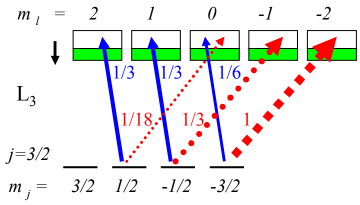

$$\left| \tfrac{3}{2}, \tfrac{3}{2} \right\rangle = \left| Y_{1,1} \uparrow \right\rangle \qquad \left| \tfrac{3}{2}, \tfrac{-3}{2} \right\rangle = \left| Y_{1,-1} \downarrow \right\rangle$$

$$\left| \tfrac{3}{2}, \tfrac{1}{2} \right\rangle = \sqrt{\tfrac{2}{3}} \left| Y_{1,0} \uparrow \right\rangle + \sqrt{\tfrac{1}{3}} \left| Y_{1,1} \downarrow \right\rangle$$

$$\left| \tfrac{3}{2}, \tfrac{-1}{2} \right\rangle = \sqrt{\tfrac{1}{3}} \left| Y_{1,-1} \uparrow \right\rangle + \sqrt{\tfrac{2}{3}} \left| Y_{1,0} \downarrow \right\rangle$$

Clesbsch-Gordan coefficients

$$Y_{lm} = \sum_{m_1 m_2} (l_1 m_1 l_2 m_2 | l, m) Y_{l_1 m_1} Y_{l_2 m_2}$$

$$Y_{l_1 m_1} Y_{l_2 m_2} = \sum_{l=|l_1 - l_2|}^{l_1 + l_2} (l_1 m_1 l_2 m_2 | lm) Y_{lm}$$

$$Y_{1,1} Y_{1,1} = Y_{2,2} \qquad Y_{1,-1} Y_{1,1} = \sqrt{\tfrac{1}{6}} Y_{2,0} + \ldots$$

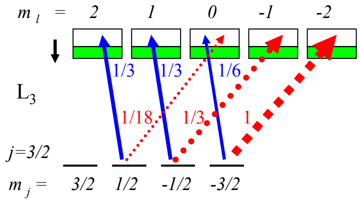

$$\sigma \propto \left|\left\langle l,m_l \middle| \boldsymbol{\varepsilon}\cdot\hat{\mathbf{r}} \middle| j,m_j\right\rangle\right|^2$$

$$\boldsymbol{\varepsilon}\cdot\hat{\mathbf{r}} = \sqrt{\tfrac{4\pi}{3}}\left(\tfrac{-\varepsilon_x+i\varepsilon_y}{\sqrt{2}}Y_{1,1}+\tfrac{\varepsilon_x+i\varepsilon_y}{\sqrt{2}}Y_{1,-1}+\varepsilon_z Y_{1,0}\right)$$

$$\sigma_\pm \propto R(r)^2\cdot\left|\left\langle Y_{lm}\middle|\frac{\varepsilon_x \mp i\varepsilon_y}{\sqrt{2}}Y_{1,\pm1}\middle| j,m_j\right\rangle\right|^2$$

$$\sigma_+ \propto \left|\left\langle Y_{2,1}\middle|\frac{\varepsilon_x - i\varepsilon_y}{\sqrt{2}}Y_{1,1}\middle| j=\tfrac{3}{2},m_j=\tfrac{-1}{2}\right\rangle\right|^2 = \tfrac{1}{3}$$

$$\because \left\langle \mathbf{Y}_{2,1}\middle|\mathbf{Y}_{1,1}\middle|\boldsymbol{j}=\tfrac{3}{2},\boldsymbol{m_j}=\tfrac{-1}{2}\right\rangle=\sqrt{\tfrac{2}{3}}\left\langle \mathbf{Y}_{2,1}\middle|\mathbf{Y}_{1,1}\middle|\mathbf{Y}_{1,0}\right\rangle=\sqrt{\tfrac{1}{3}}$$

$$Y_{1,1}Y_{1,0}=\sqrt{\tfrac{1}{2}}Y_{2,1}+.....$$

$$\sigma_- \propto \left|\left\langle Y_{2,-1}\middle|\frac{\varepsilon_x + i\varepsilon_y}{\sqrt{2}}Y_{1,-1}\middle| j=\tfrac{3}{2},m_j=\tfrac{-1}{2}\right\rangle\right|^2 = \tfrac{1}{3}$$

$$\because \left\langle \mathbf{Y}_{2,-1}\middle|\mathbf{Y}_{1,-1}\middle|\boldsymbol{j}=\tfrac{3}{2},\boldsymbol{m_j}=\tfrac{-1}{2}\right\rangle=\sqrt{\tfrac{2}{3}}\left\langle \mathbf{Y}_{2,-1}\middle|\mathbf{Y}_{1,-1}\middle|\mathbf{Y}_{1,0}\right\rangle=\sqrt{\tfrac{1}{3}}$$

$$Y_{1,-1}Y_{1,0}=\sqrt{\tfrac{1}{2}}Y_{2,-1}+.....$$

$$\left|\tfrac{3}{2},\tfrac{3}{2}\right\rangle=\left|Y_{1,1}\uparrow\right\rangle \qquad \left|\tfrac{3}{2},\tfrac{-3}{2}\right\rangle=\left|Y_{1,-1}\downarrow\right\rangle$$

$$\left|\tfrac{3}{2},\tfrac{1}{2}\right\rangle=\sqrt{\tfrac{2}{3}}\left|Y_{1,0}\uparrow\right\rangle+\sqrt{\tfrac{1}{3}}\left|Y_{1,1}\downarrow\right\rangle$$

$$\left|\tfrac{3}{2},\tfrac{-1}{2}\right\rangle=\sqrt{\tfrac{1}{3}}\left|Y_{1,-1}\uparrow\right\rangle+\sqrt{\tfrac{2}{3}}\left|Y_{1,0}\downarrow\right\rangle$$

Clesbsch-Gordan coefficients

$$Y_{lm}=\sum_{m_1m_2}(l_1m_1l_2m_2\,|\,l,m)Y_{l_1m_1}Y_{l_2m_2}$$

$$Y_{l_1m_1}Y_{l_2m_2}=\sum_{l=|l_1-l_2|}^{l_1+l_2}(l_1m_1l_2m_2\,|\,lm)Y_{lm}$$

65

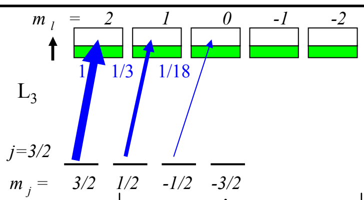

$$\sigma_+ \propto R(r)^2\cdot\left|\left\langle Y_{lm}\middle|\frac{\varepsilon_x - i\varepsilon_y}{\sqrt{2}}Y_{1,1}\middle| j,m_j\right\rangle\right|^2$$

$$\sigma_+ \propto \left|\left\langle Y_{2,2}\middle|\frac{\varepsilon_x - i\varepsilon_y}{\sqrt{2}}Y_{1,1}\middle| j=\tfrac{3}{2},m_j=\tfrac{3}{2}\right\rangle\right|^2 = 1$$

$$\because \left\langle Y_{2,2}\middle|Y_{1,1}\middle|j=\tfrac{3}{2},m_j=\tfrac{3}{2}\right\rangle=\left\langle Y_{2,1}\middle|Y_{1,1}\middle|Y_{1,1}\right\rangle=1$$

$$\sigma_+ \propto \left|\left\langle Y_{2,1}\middle|\frac{\varepsilon_x - i\varepsilon_y}{\sqrt{2}}Y_{1,1}\middle| j=\tfrac{3}{2},m_j=\tfrac{1}{2}\right\rangle\right|^2 = \tfrac{1}{3}$$

$$\because \left\langle Y_{2,1}\middle|Y_{1,1}\middle|j=\tfrac{3}{2},m_j=\tfrac{1}{2}\right\rangle=\sqrt{\tfrac{2}{3}}\left\langle Y_{2,1}\middle|Y_{1,1}\middle|Y_{1,0}\right\rangle=\sqrt{\tfrac{1}{3}}$$

$$Y_{1,1}Y_{1,0}=\sqrt{\tfrac{1}{2}}Y_{2,1}+.....$$

$$\sigma_+ \propto \left|\left\langle Y_{2,0}\middle|\frac{\varepsilon_x - i\varepsilon_y}{\sqrt{2}}Y_{1,1}\middle| j=\tfrac{3}{2},m_j=\tfrac{-1}{2}\right\rangle\right|^2 = \tfrac{1}{18}$$

$$\because \left\langle Y_{2,0}\middle|Y_{1,1}\middle|j=\tfrac{3}{2},m_j=\tfrac{1}{2}\right\rangle=\sqrt{\tfrac{1}{3}}\left\langle Y_{2,0}\middle|Y_{1,1}\middle|Y_{1,-1}\right\rangle=\sqrt{\tfrac{1}{18}}$$

$$Y_{1,1}Y_{1,-1}=\sqrt{\tfrac{1}{6}}Y_{2,0}+.....$$

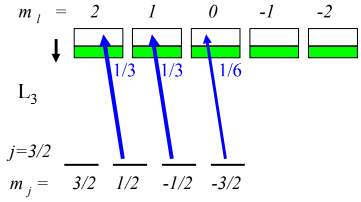

$$\left|\tfrac{3}{2},\tfrac{3}{2}\right\rangle=\left|Y_{1,1}\uparrow\right\rangle \qquad \left|\tfrac{3}{2},\tfrac{-3}{2}\right\rangle=\left|Y_{1,-1}\downarrow\right\rangle$$

$$\left|\tfrac{3}{2},\tfrac{1}{2}\right\rangle=\sqrt{\tfrac{2}{3}}\left|Y_{1,0}\uparrow\right\rangle+\sqrt{\tfrac{1}{3}}\left|Y_{1,1}\downarrow\right\rangle$$

$$\left|\tfrac{3}{2},\tfrac{-1}{2}\right\rangle=\sqrt{\tfrac{1}{3}}\left|Y_{1,-1}\uparrow\right\rangle+\sqrt{\tfrac{2}{3}}\left|Y_{1,0}\downarrow\right\rangle$$

Clesbsch-Gordan coefficients

$$Y_{lm}=\sum_{m_1m_2}(l_1m_1l_2m_2\,|\,l,m)Y_{l_1m_1}Y_{l_2m_2}$$

$$Y_{l_1m_1}Y_{l_2m_2}=\sum_{l=|l_1-l_2|}^{l_1+l_2}(l_1m_1l_2m_2\,|\,lm)Y_{lm}$$

$$Y_{1,1}Y_{1,1}=Y_{2,2} \qquad Y_{1,-1}Y_{1,1}=\sqrt{\tfrac{1}{6}}Y_{2,0}+.....$$

66